Published OnlineFirst July 3, 2014; DOI: 10.1158/1541-7786.MCR-14-0184

Chromatin, Gene, and RNA Regulation

Molecular Cancer Research

Decreased Expression of Cystathionine β-Synthase Promotes Glioma Tumorigenesis

Naoharu Takano[1,2,3], Yasmeen Sarfraz[4], Daniele M. Gilkes[1,2], Pallavi Chaturvedi[1,2], Lisha Xiang[1,2], Makoto Suematsu[3], David Zagzag[4,5], and Gregg L. Semenza[1,2,6,7,8,9,10]

Abstract

Cystathionine β-synthase (CBS) catalyzes metabolic reactions that convert homocysteine to cystathionine. To assess the role of CBS in human glioma, cells were stably transfected with lentiviral vectors encoding shRNA targeting CBS or a nontargeting control shRNA, and subclones were injected into immunodeficient mice. Interestingly, decreased CBS expression did not affect proliferation *in vitro* but decreased the latency period before rapid tumor xenograft growth after subcutaneous injection and increased tumor incidence and volume following orthotopic implantation into the caudate–putamen. In soft-agar colony formation assays, CBS knockdown subclones displayed increased anchorage-independent growth. Molecular analysis revealed that CBS knockdown subclones expressed higher basal levels of the transcriptional activator hypoxia-inducible factor 2α (HIF2α/EPAS1). HIF2α knockdown counteracted the effect of CBS knockdown on anchorage-independent growth. Bioinformatic analysis of mRNA expression data from human glioma specimens revealed a significant association between low expression of CBS mRNA and high expression of angiopoietin-like 4 (ANGPTL4) and VEGF transcripts, which are HIF2 target gene products that were also increased in CBS knockdown subclones. These results suggest that decreased CBS expression in glioma increases HIF2α protein levels and HIF2 target gene expression, which promotes glioma tumor formation.

Implications: CBS loss-of-function promotes glioma growth. *Mol Cancer Res; 12(10); 1398–406. ©2014 AACR.*

Introduction

Cystathionine β-synthase (CBS) is a metabolic enzyme that catalyzes the reaction of homocysteine with either cysteine or serine to form cystathionine and either hydrogen sulfide or water, respectively (1). A study of colon cancer reported increased CBS expression in tumor compared with adjacent normal tissue and found that shRNA-mediated silencing of CBS expression in colon cancer cell lines resulted in decreased proliferation, migration, and invasion that was attributable to decreased hydrogen sulfide production (2). In contrast, *CBS* gene expression is silenced by promoter hypermethylation in gastric cancer (3). Thus, CBS may function to either promote or suppress tumor growth, depending on the cancer cell type.

In the brain, CBS is expressed by glia and astrocytes (4), which are the cells from which gliomas arise. Neural stem cells also express CBS and the addition of the substrate L-cysteine to culture media stimulated the *in vitro* differentiation of neural stem cells to neurons and astroglia, whereas knockdown of CBS expression by siRNA suppressed L-cysteine–induced stem cell differentiation (5). Analysis of cancer stem cells from human gliomas revealed that expression of the transcriptional activator hypoxia-inducible factor 2α (HIF2α) was increased in stem cells as compared with the bulk cancer cells and that HIF2α promoted glioma stem cell self-renewal and survival (6, 7).

In this study, we analyzed the effect of CBS loss-of-function in U87-MG human glioma cells on tumor formation after subcutaneous or intracranial injection in immunodeficient mice. CBS knockdown decreased the latency time to rapid tumor xenograft growth and increased the incidence and volume of intracranial tumors. CBS knockdown also increased *in vitro* colony formation in a soft-agar

[1]Institute for Cell Engineering, Johns Hopkins University School of Medicine, Baltimore, Maryland. [2]McKusick-Nathans Institute of Genetic Medicine, Johns Hopkins University School of Medicine, Baltimore, Maryland. [3]Department of Biochemistry, School of Medicine, Keio University, Tokyo, Japan. [4]Microvascular and Molecular Neuro-Oncology Laboratory, New York University School of Medicine, New York, New York. [5]Division of Neuropathology, Department of Pathology and Neurosurgery, New York University School of Medicine, New York, New York. [6]Department of Biological Chemistry, Johns Hopkins University School of Medicine, Baltimore, Maryland. [7]Department of Medicine, Johns Hopkins University School of Medicine, Baltimore, Maryland. [8]Department of Pediatrics, Johns Hopkins University School of Medicine, Baltimore, Maryland. [9]Department of Oncology, Johns Hopkins University School of Medicine, Baltimore, Maryland. [10]Department of Radiation Oncology, Johns Hopkins University School of Medicine, Baltimore, Maryland.

Note: Supplementary data for this article are available at Molecular Cancer Research Online (http://mcr.aacrjournals.org/).

Corresponding Author: Gregg L. Semenza, Johns Hopkins University School of Medicine, Miller Research Building, Suite 671, 733 North Broadway, Baltimore, MD 21205. Phone: 410-955-1619; Fax: 443-287-5618; E-mail: gsemenza@jhmi.edu

doi: 10.1158/1541-7786.MCR-14-0184

Published OnlineFirst July 3, 2014; DOI: 10.1158/1541-7786.MCR-14-0184

assay and increased the expression of HIF2α and target genes encoding angiopoietin-like 4 (ANGPTL4) and VEGF. HIF2α knockdown counteracted the stimulatory effect of CBS knockdown on ANGPTL4 and VEGF expression as well as colony formation. In human glioma samples, decreased CBS expression was associated with increased ANGPTL4 and VEGF expression. Thus, decreased CBS expression in gliomas may promote tumorigenesis by increasing HIF2α expression.

Materials and Methods

Cell culture

U87-MG cells (8) were cultured in DMEM with 10% FBS, 100 U/mL penicillin, and 100 μg/mL streptomycin (Invitrogen) at 37°C in a humidified 5% CO_2, 95% air incubator. Hypoxic exposure was carried out in a modular incubator chamber (Billups-Rothenberg). Fresh media containing 25 mmol/L HEPES were added to the cells, the chamber was flushed with a gas mixture consisting of 1% O_2, 5% CO_2, and 94% N_2, sealed, and incubated at 37°C.

Lentivirus production and gene knockdown

Lentiviruses were produced in HEK293T cells by transfection of the following plasmids: pMD.G, pCMV-ΔR8.91, and pLKO.1 shRNA expression vector as described (9). shRNA vectors targeting CBS and shNT nontargeting control vector were purchased from Sigma. A scrambled shRNA control vector (shScr) was constructed by insertion of an oligonucleotide containing the sequence 5′-cctaaggtaagtcgcccctcg-3′ into pLKO.1. Construction of the lentiviral vector for expression of shRNA targeting HIF2α (shHIF2a#3) was described previously (9).

Tumor xenograft model

Animal protocols were in accordance with the NIH Guide for the Care and Use of Laboratory Animals and were approved by the Johns Hopkins University Animal Care and Use Committee. Mycoplasma-free U87-MG subclones were injected into 6- to 8-week-old male SCID mice. A total of 5×10^6 cells were suspended in PBS, mixed with an equal volume of Matrigel (BD Bioscience), and injected subcutaneously into the flank. Tumor size was measured with calipers twice per week. Tumor volume (mm^3) was calculated using the following formula: length (mm) × width (mm) × height (mm) × 0.52. Tumors were excised and stored at −80°C for RNA and protein extraction or fixed in 10% formalin for paraffin embedding. For IHC, paraffin sections were dewaxed, hydrated, and antigens were retrieved with citrate buffer (10 mmol/L citric acid, 2 mmol/L EDTA, 0.05% Tween-20, pH 6.2). IHC was performed with an LSAB+ System HRP Kit (Dako) and anti-CD31 (Dianova) or anti-Ki67 (Novus Biologicals) antibody.

Orthotopic injection model

Male SCID/NCr mice (6–7 weeks old) were maintained in accordance with a protocol approved by the New York University Institutional Animal Care and Use Committee (New York, NY). U87-MG subclones were implanted stereotactically into mouse brains. Mice were anesthetized by intraperitoneal injection with xylazine chloride hydrate (10 mg/kg) and ketamine (90 mg/kg) and a burr hole was drilled into the skull 0.1 mm posterior to the bregma and 2.3 mm lateral to the midline. U87-MG cells in 2 μL of medium were injected using a stereotactic head frame (David Kopf Instruments) in the defined location of the caudate/putamen using a 10-μL Hamilton syringe with a 1-inch 30-gauge needle attached and inserted into a Kopf microinjection unit (Model 5000 with Model 5001 Hamilton syringe holder). The needle was advanced to a depth of 2.35 mm from the cortical surface and the cell suspension was delivered over 3 to 4 minutes. Following injection, the needle was left in place for 2 minutes, then raised to a depth of 1.5 mm below the dura and left in place for an additional minute. Upon withdrawal of the needle, the burr hole was filled with bone wax and the incision sutured. On day 36, mice were anesthetized, perfused intracardially with PBS followed by 4% paraformaldehyde, and brains were harvested and placed in cold 4% paraformaldehyde overnight, followed by paraffin embedding. Tumor volume was calculated from hematoxylin- and eosin-stained sections using the formula: $L \times S^2 \times 1/2$, where L and S are the long and short axes of the tumor. Depth of invasion was assessed as previously described (10).

IHC was performed on paraformaldehyde-fixed, paraffin-embedded, 4-μm sections using goat anti-mouse CD105/Endoglin (R&D Systems), rabbit anti-mouse/human cleaved caspase-3 (Cell Signaling Technology), or rabbit anti-mouse/human Ki67 (Thermo Scientific). For CD105 and Ki67, sections were deparaffinized, rehydrated, epitope retrieval was performed in a 1,200 Watt microwave oven at 100% power in 10 mmol/L sodium citrate buffer, pH 6.0 for 20 minutes, and detection was carried out at 40°C on a NexES instrument (Ventana Medical Systems) using reagent buffer and detection kits from Ventana unless otherwise noted. For cleaved caspase-3, the Discovery XT instrument (Ventana Medical Systems) was used with online deparaffinization and antigen retrieval in citrate buffer for 32 minutes. Endogenous peroxidase activity was blocked with hydrogen peroxide. Antibodies were diluted in Dulbecco's PBS (Life Technologies) as follows: CD105, 1:200; Ki67, 1:400; and cleaved caspase-3, 1:100. CD105 samples were incubated overnight at room temperature, whereas Ki67 and cleaved caspase-3 sections were incubated at 40°C for 30 minutes and 4 hours, respectively. CD105 and Ki67 were detected with biotinylated horse anti-goat diluted 1:100 and biotinylated goat anti-rabbit diluted 1:200 (Vector Laboratories), respectively, followed by application of streptavidin-horseradish peroxidase (HRP) conjugate. Cleaved caspase-3 was detected using anti-rabbit multimer (HRP). The complex was visualized with 3,3 diaminobenzidene and enhanced with copper sulfate. Slides were washed in distilled water, counterstained with hematoxylin, dehydrated and mounted with permanent media. Appropriate positive and negative controls were included with the study sections.

Published OnlineFirst July 3, 2014; DOI: 10.1158/1541-7786.MCR-14-0184

Soft-agar assay

Twenty-five hundred U87-MG cells were suspended in 0.3% top agar and plated on 0.6% bottom agar. Both agar layers contained DMEM supplemented with 10% FBS, 100 U/mL penicillin, and 100 μg/mL streptomycin. Plates were incubated for 3 to 4 weeks at 37°C in a humidified 5% CO_2, 95% air incubator.

Reverse transcription and qRT-PCR

Total RNA was isolated with TRIzol (Invitrogen), treated with DNase I (Ambion), and cDNA was synthesized using the iScript cDNA Synthesis Kit (Bio-Rad). qPCR was performed using SYBR Green (Bio-Rad). The target mRNA expression was calculated, relative to 18S rRNA levels in the same sample, based on the $\Delta(\Delta C_t)$ method: $\Delta C_t = Ct_{target} - Ct_{18S}$; $\Delta(\Delta C_t) = Ct_{test\text{-}subclone} - Ct_{control\text{-}subclone}$. Primer sequences are listed on Supplementary Table S1.

Immunoblot assays

Whole-cell lysates and tissue lysates were prepared in modified RIPA buffer [25 mmol/L Tris-HCl (pH 7.6), 150 mmol/L NaCl, 1% IGEPAL CA-630, 1% Sodium deoxycholate, 0.1% SDS) supplemented with protease inhibitors (Roche). Antibodies against following proteins were used: HIF1α (BD Biosciences), HIF2α (Novus Biologicals), CBS (Abnova), and Actin (Santa Cruz Biotechnology).

Statistical analysis

Data from U87-MG subclones were compared by Student *t* test or analysis of variation, before data normalization. Gene expression profiles from human brain cancers (11) were obtained from the Gene Expression Omnibus (GEO) database (GSE4290). To analyze the correlation between CBS and VEGF or ANGPTL4 mRNA expression, Pearson correlation coefficient (*r*) was determined and the associated *P* value was calculated using GraphPad Prism software.

Results

CBS loss-of-function decreases tumor xenograft latency

To assess the role of CBS in glioma tumorigenesis, we established a U87-MG subclone, designated shCBS#07 that stably expressed an shRNA designed to inhibit CBS expression, which is induced by hypoxia in U87-MG cells (9). Thus, parental U87-MG and shCBS#07 cells were exposed to 20% or 1% O_2 for 3 days and CBS expression was analyzed by an immunoblot assay. CBS expression was induced by hypoxia in parental cells but not in the shCBS#07 subclone (Fig. 1A).

To evaluate the role of CBS in tumorigenesis, parental U87-MG and shCBS#07 cells were subcutaneously injected into the flank of SCID mice. Although the latency period before rapid tumor growth after injection of parental U87-MG cells was 3 weeks, rapid tumor growth was observed less than 2 weeks after injection of the shCBS#07 subclone. When the tumors were harvested 5 weeks after injection, the parental tumors had reached a mean volume of 600 mm^3 and weight of 0.5 g, whereas the shCBS#07 tumors were 1500 mm^3 and 1.7 g (Fig. 1B and C). IHC analysis of tumor sections was performed with an antibody against CD31 and the number of $CD31^+$ blood vessels was counted. As shown in Fig. 1D, shCBS#07 tumors had a significantly higher vessel density than parental tumors. Ki67 IHC revealed that there was no significant difference in cell proliferation between parental and shCBS#07 tumors (Fig. 1E), which was consistent with the similar tumor growth rates by the end of the experiment (Fig. 1B). Consistent with the increased vessel density, the expression of mRNAs encoding three angiogenic growth factors, VEGF, angiopoietin 2, and ANGPTL4, was significantly increased in shCBS#07 tumors as compared with parental tumors, whereas expression of placental growth factor and stromal-derived factor 1 was similar between subclones (Fig. 1F).

To establish that the difference in tumorigenesis between the cell lines was specifically due to CBS loss-of-function, two additional subclones were generated (Fig. 2A). One subclone expressed an shRNA that targeted a different sequence in CBS mRNA (shCBS#61). The other subclone expressed a scrambled shRNA sequence that did not target CBS (shScr). There was no significant difference between subclones with respect to *in vitro* cell proliferation at either 20% or 1% O_2 (Supplementary Fig. S1). We hypothesized that the increased angiogenesis in shCBS#07 tumors was a reflection of their more advanced growth due to the decreased latency period. To test this hypothesis, rather than harvesting tumors at the same time point, tumors were harvested when they reached a volume of 1,000 mm^3 (Fig. 2B and C). As in the previous experiment, after subcutaneous injection the subclones with CBS expression (parental and shScr) showed a latency period of 3 weeks and reached 1,000 mm^3 by 7 to 7.5 weeks after injection, whereas the subclones with CBS loss-of-function showed a latency period of less than 2 weeks and reached 1,000 mm^3 within 4.5 to 5 weeks; however, by the end of the experiment, the growth rates were identical in all four subclones (Fig. 2B). The tumors were harvested and analyzed by qRT-PCR, which demonstrated a significant decrease in CBS mRNA levels in shCBS#07 and shCBS#61 tumors compared with parental and shScr tumors (Fig. 2D). Although shCBS#07 tumors had higher vessel density than parental U87-MG cells when they were harvested at the same time point (Fig. 1D), parental, shScr, shCBS#07, and shCBS#61 tumors had similar vessel density when they were harvested at the same tumor volume (Fig. 2E). The parallel late-stage tumor growth curves (Fig. 2B) and absence of any difference in Ki67 staining (Fig. 1E) suggest that the tumor-promoting effect of CBS deficiency occurs early in tumorigenesis.

CBS loss-of-function increases tumor incidence and volume after orthotopic transplantation

Because the consequences of gene knockdown in a mouse model of astrocytoma were found to differ dramatically after subcutaneous as compared with orthotopic transplantation (12), we performed orthotopic injection of parental U87-MG and shCBS#07 cells as well as a subclone expressing a

Published OnlineFirst July 3, 2014; DOI: 10.1158/1541-7786.MCR-14-0184

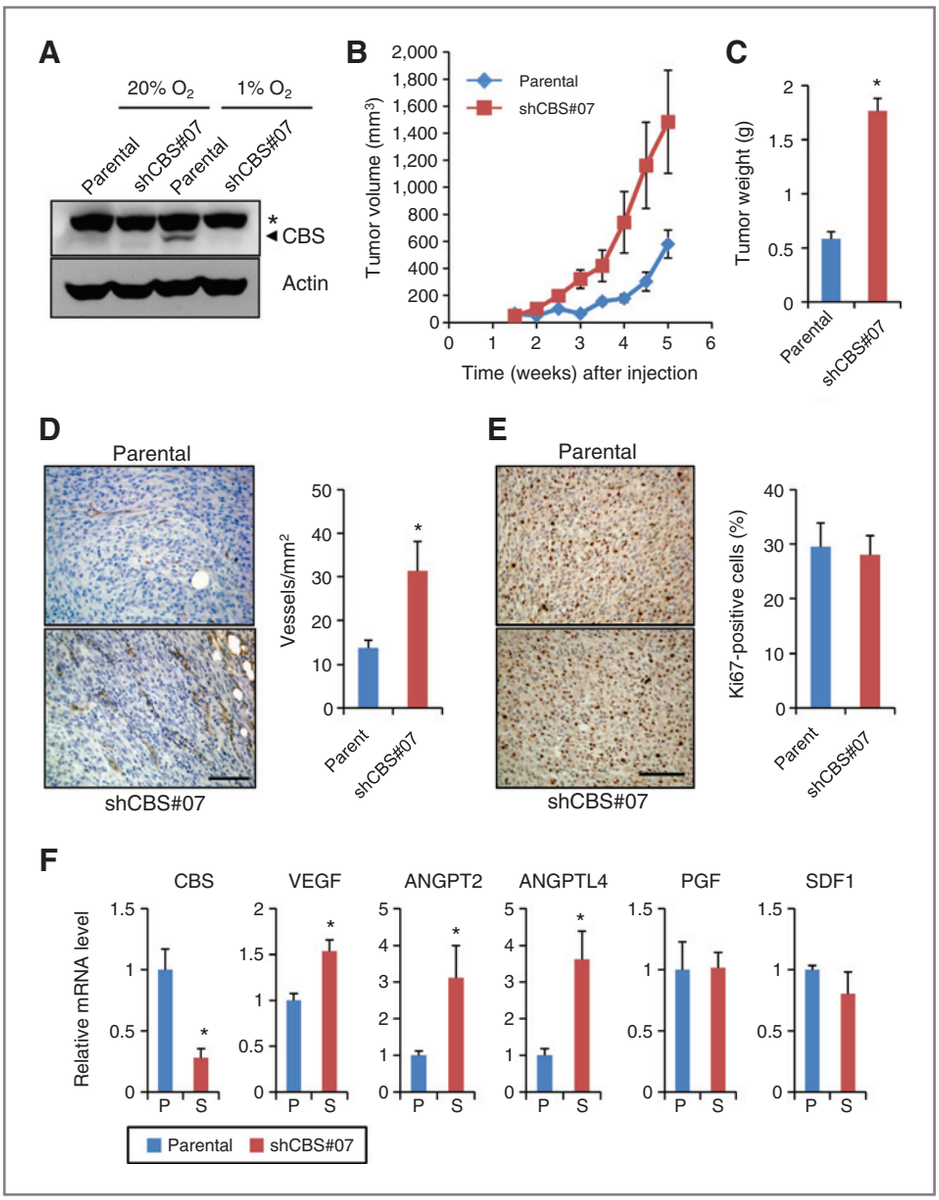

Figure 1. Effect of CBS knockdown on the growth of U87-MG tumor xenografts. A, U87-MG subclones were exposed to 1% or 20% O_2 for 3 days and immunoblot assays were performed to analyze CBS and actin protein levels. Asterisk indicates a nonspecific band and arrowhead points to CBS-specific band. B, parental and CBS knockdown U87-MG cells were injected subcutaneously into the flank of SCID mice and tumor volume was determined (mean ± SEM, $n = 4$) by serial caliper measurements. C, tumors were harvested at 5.5 weeks after injection and weight was determined (mean ± SEM, $n = 4$); *, $P < 0.05$ versus parental. D, anti-CD31 IHC and hematoxylin counterstaining were performed (left; scale bar, 100 μm) and blood vessel density in tumor sections was determined (right; mean ± SEM, $n = 8$); *, $P < 0.05$. E, anti Ki67 IHC and hematoxylin counterstaining were performed (left; scale bar, 100 μm) to quantify $Ki67^+$ proliferating cells in tumors derived from injection of parental U87-MG cells and shCBS#07 subclone (right; mean ± SEM, $n = 8$). F, levels of mRNAs encoding CBS and angiogenic growth factors in harvested tumor samples were determined by reverse transcription and qRT-PCR and normalized to the parental samples (mean ± SEM, $n = 4$); *, $P < 0.05$.

nontargeting shRNA (shNT). Five weeks after injection of 1×10^5 cells into the brains of SCID mice, the brains were harvested and scored for the presence and volume of tumor tissue. All 7 mice that were injected with shCBS#07 cells formed tumors, whereas tumors formed in only 4 out of 7 mice injected with parental cells and 3 out of 7 mice injected with shNT cells. Consistent with data from the subcutaneous injection model, the mean volume of shCBS#07 tumors was significantly greater than parental tumors (Fig. 3A), whereas there was no significant difference with respect to depth of invasion into the brain (Fig. 3B) or vascular density (Fig. 3C). In addition, by the end of the experiment there was no significant difference with respect to proliferation, as determined by Ki67 IHC (Fig. 3D), or apoptosis, as determined by IHC using an antibody specific for cleaved caspase-3, which revealed low levels of apoptosis in all tumor sections (Fig. 3E).

Because the major difference observed was with respect to tumor incidence, we repeated the experiment, but this time injected a 10-fold lower number of cells (i.e., 1×10^4). Again, tumors formed in all 7 mice injected with shCBS#07, whereas tumors formed in only 5 out of 7 mice injected with shNT cells, and 6 out of 7 mice injected with parental U87-MG cells. We also assessed tumor volume, depth of invasion, vascular density, cell proliferation, and cell apoptosis and again observed a significant difference only with respect to tumor volume (Supplementary Fig. S2). Taken together, the xenotopic and orthotopic models indicate that CBS loss-of-function increases tumorigenicity.

Published OnlineFirst July 3, 2014; DOI: 10.1158/1541-7786.MCR-14-0184

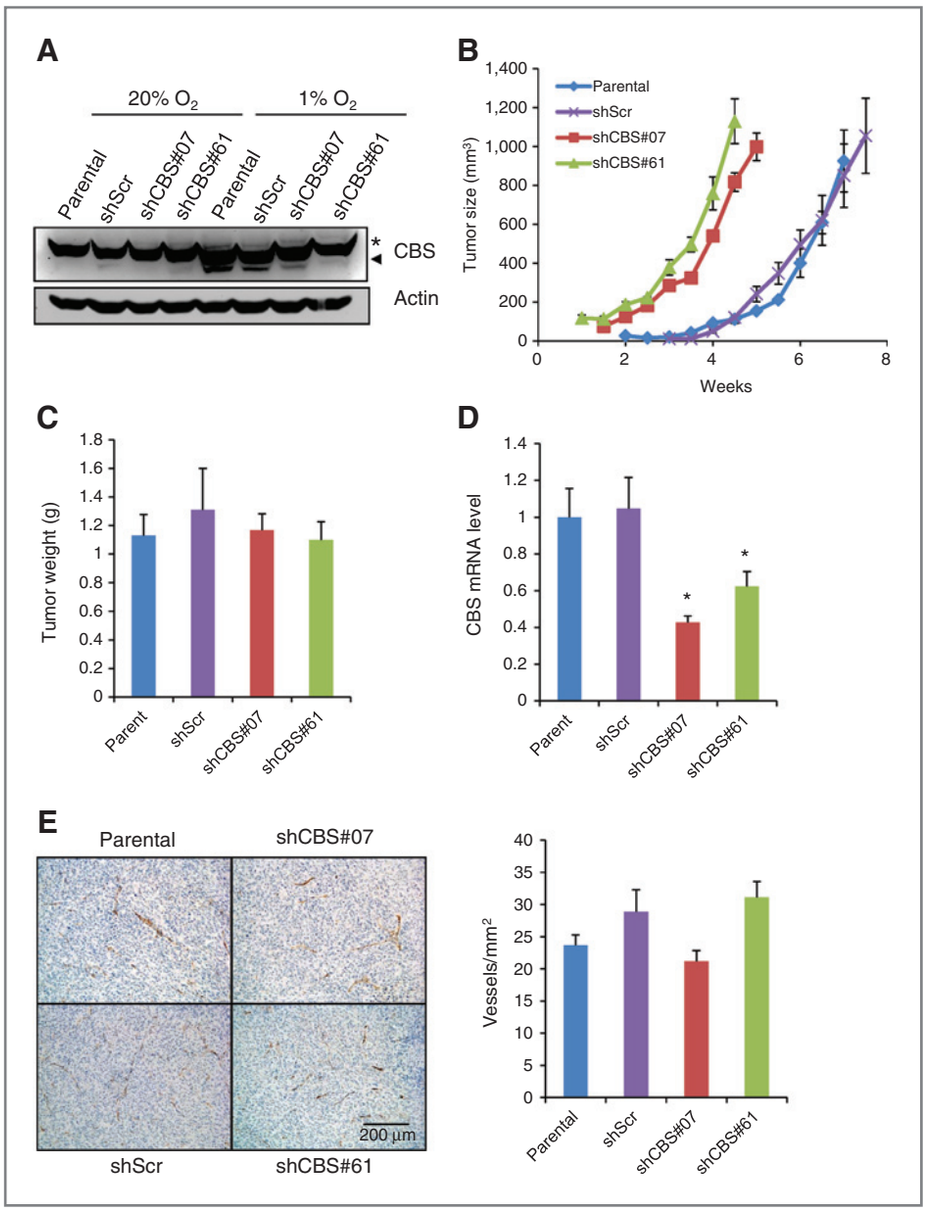

Figure 2. Analysis of 1,000 mm^3 tumor xenografts derived from subcutaneous injection of U87-MG subclones. A, immunoblot assays were performed to analyze CBS and actin protein levels in lysates of U87-MG subclones that were cultured under 1% or 20% O_2 for 3 days. Asterisk indicates a nonspecific band and arrowhead points to CBS-specific band. B, U87-MG subclones were injected subcutaneously into the flank of SCID mice and tumors were harvested when they reached a volume of 1,000 mm^3 (mean ± SEM, $n = 4$). C, the harvested tumors were weighed (mean ± SEM, $n = 4$). D, CBS mRNA levels in tumor samples were determined by qRT-PCR and normalized to the parental samples (mean ± SEM, $n = 4$); *, $P < 0.05$ versus shScr. E, anti-CD31 IHC and hematoxylin counterstaining of tumor sections (left; scale bar, 0.2 mm) were performed to determine blood vessel density (right; mean ± SEM, $n = 8$).

CBS loss-of-function increases anchorage-independent cell growth

Immediately after injection, cancer cells are in an anchorage-independent state in which they are detached from extracellular matrix, which can trigger a form of programmed cell death known as anoikis (13). Anchorage-independent cell growth can be investigated by analyzing colony formation in soft agar. As shown in Fig. 4A, shCBS#07 and shCBS#61 cells formed a significantly greater number of colonies in soft agar as compared with parental U87-MG or shScr cells. ANGPTL4 and VEGF have been reported to promote anchorage-independent growth and protect against anoikis in cancer cells (14, 15). VEGF and ANGPTL4 mRNA levels were significantly higher in the two CBS-deficient subclones than in parental and shScr cells (Fig. 4B).

To determine the clinical relevance of these observations, we investigated whether CBS mRNA levels were correlated with VEGF or ANGPTL4 mRNA levels in 180 primary patient-derived gliomas by interrogating a microarray dataset in the GEO database (GSE4290; ref. 7). As shown in Fig. 4C, CBS mRNA levels showed negative correlations with VEGF and ANGPTL4 mRNA levels that were statistically significant ($P < 0.01$). These results suggest that CBS expression negatively regulates VEGF and ANGPTL4 expression in human glioma.

CBS deficiency increases HIF2α expression and anchorage-independent cell growth

Expression of ANGPTL4 (16) and VEGF (17) is regulated by HIFs in cancer cells and H_2S has been reported to

Published OnlineFirst July 3, 2014; DOI: 10.1158/1541-7786.MCR-14-0184

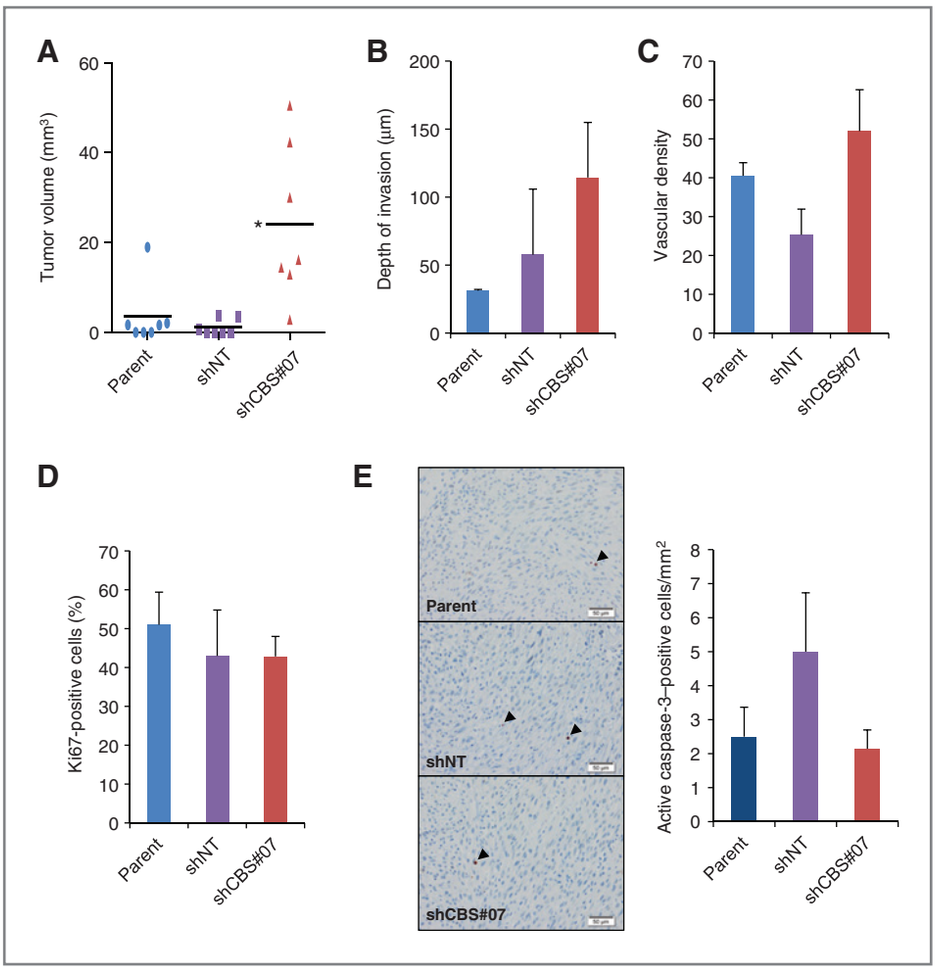

Figure 3. Analysis of orthotopic tumors. A, tumor volume was measured 5 weeks after stereotactic injection of U87-MG subclones into the brains of SCID mice (bar, mean; $n = 7$); *, $P < 0.05$ versus shNT. B, depth of invasion was measured from brain tumor sections (mean ± SEM, $n = 3$–6). C, anti-CD105 IHC was performed and vessel density in tumor sections was determined (mean ± SEM, $n = 6$–14). D, anti-Ki67 IHC was performed and Ki67$^+$ cells were counted (mean ± SEM, $n = 3$–7). E, immunohistochemistry was performed (left; scale bar, 50 μm) with an antibody that selectively recognizes cleaved (active) caspase-3 (arrowheads). Positive cells were counted (right; mean ± SEM; $n = 3$–7).

inhibit HIF1α protein expression *in vitro* (18, 19), suggesting that CBS loss-of-function might increase HIF-dependent ANGPTL4 and VEGF expression. To test this hypothesis, we analyzed HIF1α and HIF2α protein levels in U87-MG subclones that were exposed to 20% or 1% O_2 for 3 days. Immunoblot assays revealed no consistent difference in HIF1α protein levels between control and CBS-deficient subclones, whereas HIF2α protein levels were increased in CBS-deficient subclones under nonhypoxic conditions (Fig. 5A). Densitometric analysis of HIF2α immunoblot band intensity in lysates prepared from five replicate cultures of shScr and shCBS#07 subclones incubated at 20% O_2 confirmed that HIF2α levels were significantly higher in shCBS#07 cells (Fig. 5B). In contrast, HIF2α mRNA levels were not increased in CBS-deficient subclones (Supplementary Fig. S3), indicating an effect on HIF2α protein synthesis or stability.

We next stably transfected parental U87-MG cells and the shCBS#07 subclone with an shRNA targeting HIF2α (shHIF2α#3), which efficiently reduced HIF2α protein levels in both subclones (Fig. 5C). VEGF and ANGPTL4 mRNA levels were significantly reduced in these HIF2α-deficient subclones (Fig. 5D). Soft-agar assays revealed that the increase in colony formation associated with CBS deficiency was lost when HIF2α expression was also silenced (Fig. 5E). Taken together, the data presented in Fig. 5 indicate that decreased CBS expression results in increased HIF2α protein levels, which stimulate ANGPTL4 and VEGF expression, leading to increased anchorage-independent growth, thereby providing a potential explanation for the increased tumorigenicity of the CBS-deficient subclones.

Discussion

In this study, we found that shRNA-dependent inhibition of CBS in U87-MG glioma cells increased tumor xenograft growth by decreasing the latency period before exponential growth. CBS also increased the incidence and volume of brain tumors after orthotopic injection, without affecting tumor cell proliferation, which is also consistent with a decreased latency period. CBS deficiency did not affect the *in vitro* proliferation of adherent U87-MG cells, but significantly increased colony formation in soft-agar assays of anchorage-independent growth. Taken together, the results of both *in vivo* and *in vitro* assays suggest that reduced CBS

Published OnlineFirst July 3, 2014; DOI: 10.1158/1541-7786.MCR-14-0184

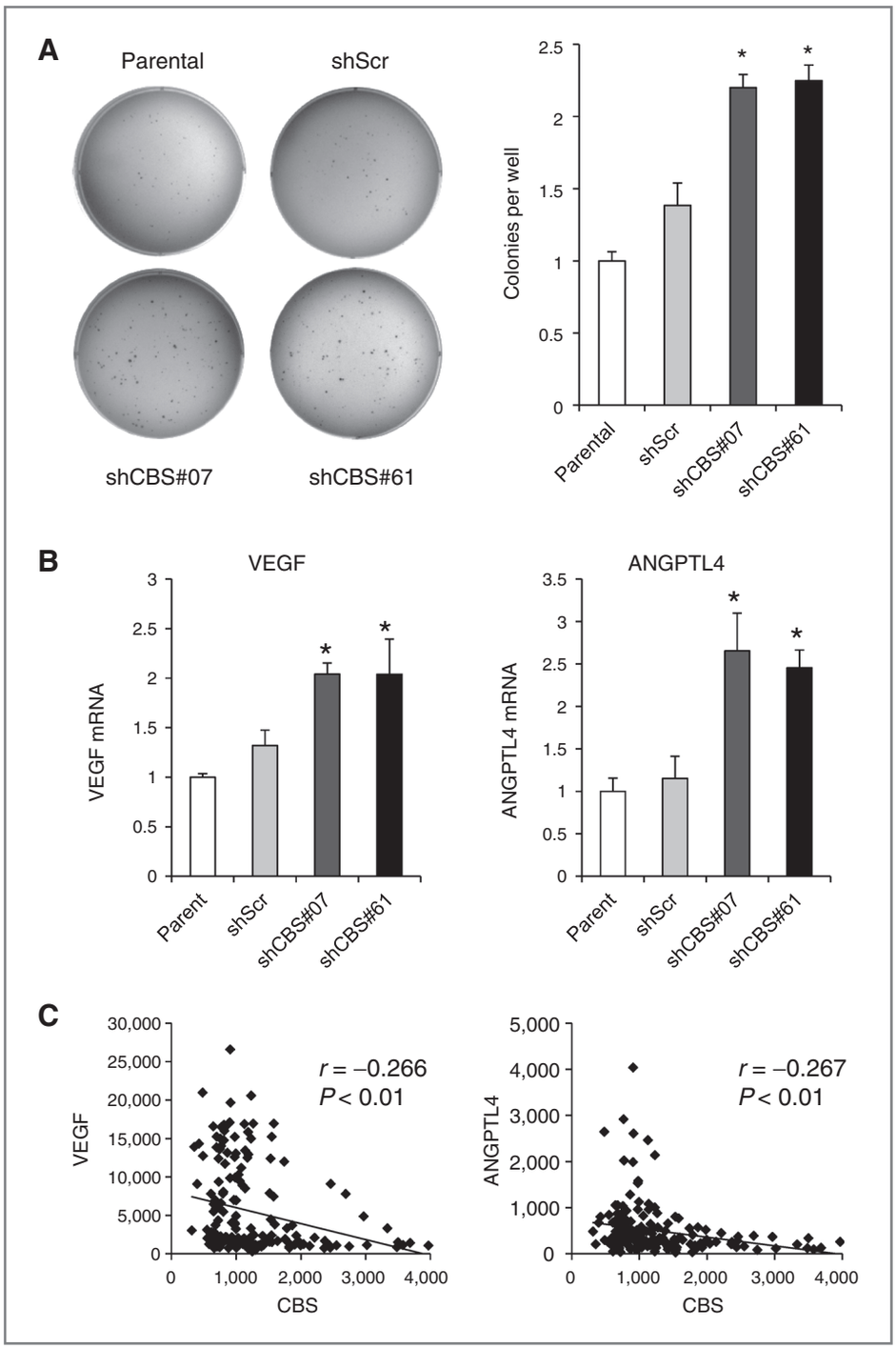

Figure 4. Analysis of colony formation in soft agar and gene expression in U87-MG subclones and patient-derived glioma tissue. A, U87-MG subclones were grown in soft agar (left), colonies were counted, and normalized to the parental cells (right; mean ± SEM, $n = 6$); *, $P < 0.05$ versus shScr. B, VEGF (left) and ANGPTL4 (right) mRNA expression in U87-MG subclones cultured at 20% O_2 were determined by qRT-PCR and normalized to the parental samples (mean ± SEM, $n = 3$); *, $P < 0.05$ versus shScr. C, the signal intensity for CBS versus VEGF (left) or CBS versus ANGPTL4 (right) mRNA microarray data obtained from 180 patient-derived glioma samples in the GEO database (GSE4290) was plotted. For each plot, the Pearson *r* statistic and derived *P* value are shown.

expression promotes glioma tumorigenesis. Here, we use the term tumorigenesis to emphasize that the effect of CBS deficiency occurs at an early step in the process of tumor formation and is not due to intrinsic differences in cell proliferation. Tumorigenesis should be distinguished from carcinogenesis, the process of mutation and selection, which does not occur when U87-MG cells are transplanted into mice.

Molecular analyses indicated that CBS knockdown was associated with increased HIF2α protein expression and HIF2α-dependent expression of ANGPTL4 and VEGF, which have been shown to protect against anoikis in other cancer cell lines (14, 15), providing a potential, but currently unproven, mechanism for the increased tumorigenicity of CBS-deficient subclones, although increased HIF2α protein levels may have affected the expression of multiple HIF

Published OnlineFirst July 3, 2014; DOI: 10.1158/1541-7786.MCR-14-0184

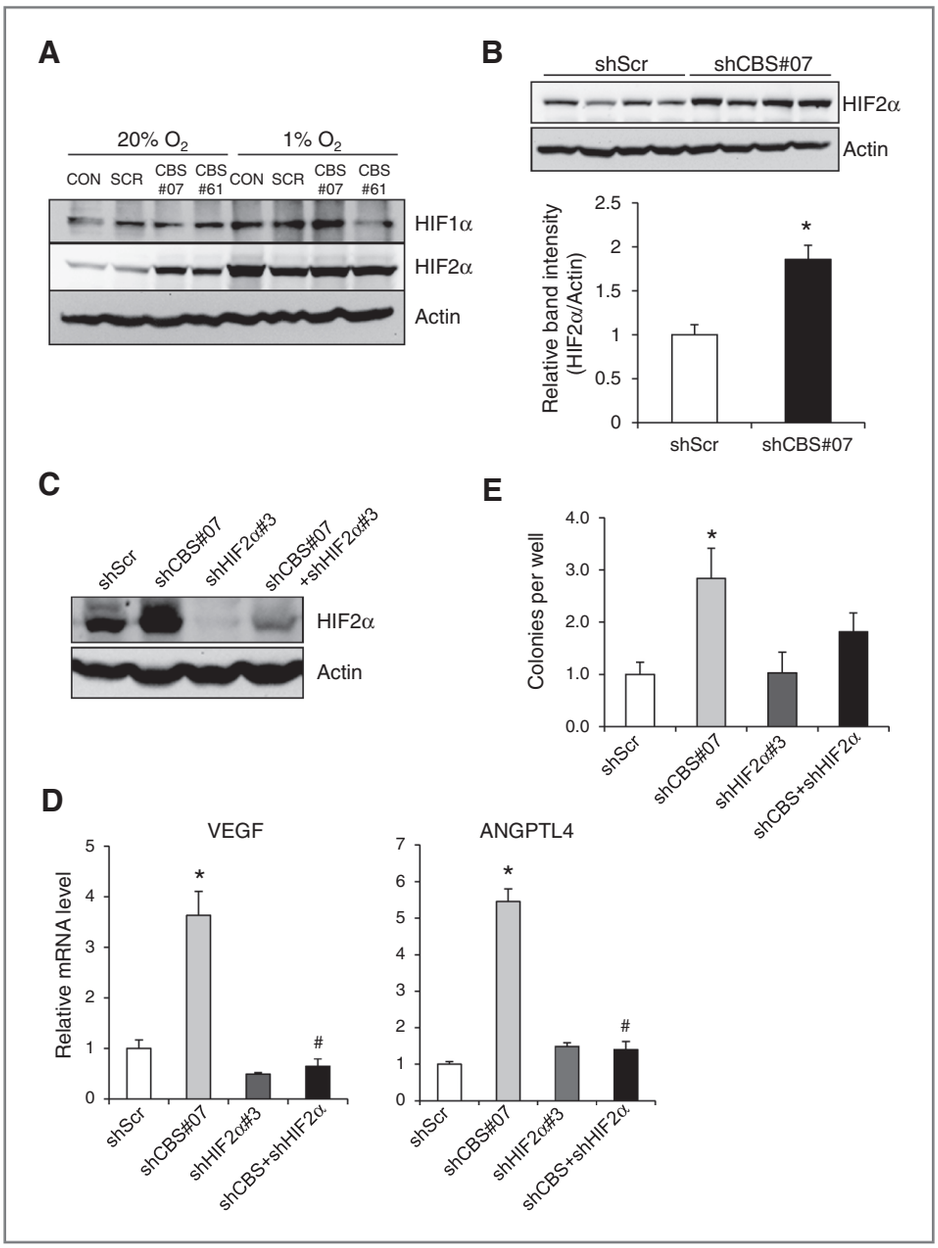

Figure 5. Analysis of HIF2α expression in U87-MG subclones. A, immunoblot assays were performed to analyze HIF1α, HIF2α, and actin protein levels in lysates from U87-MG subclones that were exposed to 1% or 20% O_2 for 3 days. B, immunoblot assays were performed to analyze HIF2α expression in five replicate cultures of shScr and shCBS#07 subclones cultured at 20% O_2 for 3 days (top). Densitometry was performed and the ratio of HIF2α: actin band intensity was determined (bottom; mean ± SEM, $n = 4$); *, $P < 0.05$. C, immunoblot assays were performed to analyze HIF2α levels in shScr, shCBS#07, shHIF2α#3, and shCBS#07+HIF2α#3 subclones cultured under 20% O_2. D, VEGF (left) and ANGPTL4 (right) mRNA levels in shScr, shCBS#07, shHIF2α#3, and shCBS#07+shHIF2α#3 subclones cultured under 20% O_2 were determined by qRT-PCR and normalized to shScr (mean ± SEM, $n = 3$); *, $P < 0.05$ versus shScr; #, $P < 0.05$ versus shCBS#07. E, colony formation ability of U87-MG subclones was measured by soft-agar assay and normalized to shScr (mean ± SEM, $n = 4$); *, $P < 0.05$ versus shScr.

target genes (20). It should be noted that although expression of the *ANGPTL4* and *VEGF* genes is regulated by both HIF1 and HIF2, increased expression of these genes in CBS-deficient U87-MG cells appears to be due specifically to increased HIF2α protein levels.

Two prior studies demonstrated that treatment of various human cancer cell lines with H_2S donors inhibited HIF1α protein expression, but one group implicated changes in HIF1α and HIF2α stability (18), whereas the other group reported effects on HIF1α synthesis (19), and it is uncertain whether data obtained by pharmacologic treatment of cell lines is physiologically relevant. If CBS loss-of-function in U87-MG cells was associated with changes in H_2S production, it is not clear why only HIF2α expression was affected by CBS knockdown, although it should be noted that CBS activity impacts on other metabolic pathways, including those affecting protein and DNA methylation (1, 21). Thus, extensive additional studies may be required to resolve this issue.

CBS expression was negatively correlated with ANGPTL4 and VEGF mRNA levels in 180 patient-derived glioma samples, which suggests that the findings from our analysis of U87-MG cells are clinically relevant. Further studies are required to determine whether CBS expression in gliomas is repressed by promoter hypermethylation as reported for gastric carcinoma (3).

Published OnlineFirst July 3, 2014; DOI: 10.1158/1541-7786.MCR-14-0184

Disclosure of Potential Conflicts of Interest

No potential conflicts of interest were disclosed.

Authors' Contributions

Conception and design: N. Takano, D. Zagzag, G.L. Semenza
Development of methodology: N. Takano, P. Chaturvedi, D. Zagzag
Acquisition of data (provided animals, acquired and managed patients, provided facilities, etc.): N. Takano, Y. Sarfraz, D. Zagzag
Analysis and interpretation of data (e.g., statistical analysis, biostatistics, computational analysis): N. Takano, Y. Sarfraz, D.M. Gilkes, L. Xiang, D. Zagzag, G.L. Semenza
Writing, review, and/or revision of the manuscript: N. Takano, M. Suematsu, D. Zagzag, G.L. Semenza
Administrative, technical, or material support (i.e., reporting or organizing data, constructing databases): N. Takano, D. Zagzag
Study supervision: D. Zagzag, G.L. Semenza

Acknowledgments

The authors thank Karen Padgett (Novus Biologicals) for generously providing antibodies against HIF2α and Ki67, Maimon Hubbi (Johns Hopkins University School of Medicine) for helpful discussions, and the Histopathology and Immunohistochemistry Core of the NYU Cancer Institute.

Grant Support

This work was supported in part by the Japan Science and Technology Agency Exploratory Research for Advanced Technology Office and funds from the Johns Hopkins Institute for Cell Engineering. The Histopathology and Immunohistochemistry Core of the NYU Cancer Institute is supported in part by NIH grant P30-CA016087.

The costs of publication of this article were defrayed in part by the payment of page charges. This article must therefore be hereby marked *advertisement* in accordance with 18 U.S.C. Section 1734 solely to indicate this fact.

Received April 7, 2014; revised May 27, 2014; accepted June 11, 2014; published OnlineFirst July 3, 2014.

References

1. Kajimura M, Fukuda R, Bateman RM, Yamamoto T, Suematsu M. Interactions of multiple gas-transducing systems: hallmarks and uncertainties of CO, NO, and H_2S gas biology. Antioxid Redox Signal 2010;13:157–92.
2. Szabo C, Coletta C, Chao C, Modis K, Szczesny B, Papapetropoulos A, et al. Tumor-derived hydrogen sulfide, produced by cystathionine β-synthase, stimulates bioenergetics, cell proliferation, and angiogenesis in colon cancer. Proc Natl Acad Sci U S A 2013;110:12474–9.
3. Zhao H, Li Q, Wang J, Su W, Ng KM, Qiu T, et al. Frequent epigenetic silencing of the folate-metabolizing gene cystathionine β−synthase in gastrointestinal cancer. PLoS ONE 2012;7:e49683.
4. Morikawa T, Kajimura M, Nakamura T, Hishiki T, Nakanishi T, Yukutake Y, et al. Hypoxic regulation of the cerebral microcirculation is mediated by a carbon monoxide-sensitive hydrogen sulfide pathway. Proc Natl Acad Sci U S A 2012;109:1293–8.
5. Wang Z, Liu D, Wang F, Zhang Q, Du Z, Zhan J, et al. L-cysteine promotes the proliferation and differentiation of neural stem cells via the CBS/H_2S pathway. Neuroscience 2013;237:106–17.
6. Li Z, Bao S, Wu Q, Wang H, Eyler C, Sathornsumetee S, et al. Hypoxia-inducible factors regulate the tumorigenic capacity of glioma stem cells. Cancer Cell 2009;15:501–13.
7. Seidel S, Garvalov BK, Wirta V, von Stechow L, Schänzer A, Meletis K, et al. A hypoxic niche regulates glioblastoma stem cells through hypoxia-inducible factor 2α. Brain 2010;133:983–95.
8. Pontén J, Macintyre EH. Long term culture of normal and neoplastic human glia. Acta Pathol Microbiol Scand 1968;74:465–86.
9. Takano N, Peng YJ, Kumar GK, Luo W, Hu H, Shimoda LA, et al. Hypoxia-inducible factors regulate human and rat cystathionine β-synthase gene expression. Biochem J 2014;458:203–11.
10. Mendez O, Zavadil J, Esencay M, Lukyanov Y, Santovasi D, Wang SC, et al. Knock down of HIF-1α in glioma cells reduces migration *in vitro* and invasion *in vivo* and impairs their ability to form tumor spheres. Mol Cancer 2010;9:133.
11. Sun L, Hui AM, Su Q, Vortmeyer A, Kotliarov Y, Pastorino S, et al. Neuronal and glioma-derived stem cell factor induces angiogenesis within the brain. Cancer Cell 2006;9:287–300.
12. Blouw B, Song H, Tihan T, Bosze J, Ferrara N, Gerber HP, et al. The hypoxic response of tumors is dependent on their microenvironment. Cancer Cell 2003;4:133–46.
13. Paoli P, Giannoni E, Chiarugi P. Anoikis molecular pathways and its role in cancer progression. Biochim Biophys Acta 2013;1833:3481–98.
14. Zhu P, Tan MJ, Huang RL, Tan CK, Chong HC, Pal M, et al. Angiopoietin-like 4 protein elevates the prosurvival intracellular O_2(-):H_2O_2 ratio and confers anoikis resistance to tumors. Cancer Cell 2011;19:401–15.
15. Desai S, Laskar S, Pandey BN. Autocrine IL-8 and VEGF mediate epithelial-mesenchymal transition and invasiveness via p38/JNK-ATF-2 signalling in A549 lung cancer cells. Cell Signal 2013;25:1780–91.
16. Zhang H, Wong CC, Wei H, Gilkes DM, Korangath P, Chaturvedi P, et al. HIF-1-dependent expression of angiopoietin-like 4 and L1CAM mediates vascular metastasis of hypoxic breast cancer cells to the lungs. Oncogene 2012;31:1757–70.
17. Forsythe JA, Jiang BH, Iyer NV, Agani F, Leung SW, Koos RD, et al. Activation of vascular endothelial growth factor gene transcription by hypoxia-inducible factor 1. Mol Cell Biol 1996;16:4604–13.
18. Kai S, Tanaka T, Daijo H, Harada H, Kishimoto S, Suzuki K, et al. Hydrogen sulfide inhibits hypoxia- but not anoxia-induced hypoxia-inducible factor 1 activation in a von Hippel-Lindau- and mitochondria-dependent manner. Antioxid Redox Signal 2012;16:203–16.
19. Wu B, Teng H, Yang G, Wu L, Wang R. Hydrogen sulfide inhibits the translational expression of hypoxia-inducible factor-1α. Br J Pharmacol 2012;167:1492–505.
20. Semenza GL. Hypoxia-inducible factors: mediators of cancer progression and targets for cancer therapy. Trends Pharmacol Sci 2012;33:207–14.
21. Yamamoto T, Takano N, Ishiwata K, Ohmura M, Nagahata Y, Matsuura T, et al. Reduced methylation of PFKFB3 in cancer cells shunts glucose towards the pentose phosphate pathway. Nat Commun 2014;5:3480.

Published OnlineFirst July 3, 2014; DOI: 10.1158/1541-7786.MCR-14-0184

Molecular Cancer Research

Decreased Expression of Cystathionine β-Synthase Promotes Glioma Tumorigenesis

Naoharu Takano, Yasmeen Sarfraz, Daniele M. Gilkes, et al.

Mol Cancer Res 2014;12:1398-1406. Published OnlineFirst July 3, 2014.